

Nonlinear wave collapse, shock, and breather formation in an electron magnetohydrodynamic plasma

Samiran Ghosh

Department of Applied Mathematics, University of Calcutta, 92, Acharya Prafulla Chandra Road, Kolkata-700009, India

Nikhil Chakrabarti

Saha Institute of Nuclear Physics, 1/AF Bidhannagar Kolkata-700064, India

(Received 1 September 2014; revised manuscript received 6 November 2014; published 17 December 2014)

Low-frequency nonlinear wave dynamics is investigated in a two-dimensional inhomogeneous electron magnetohydrodynamic (EMHD) plasma in the presence of electron viscosity. In the long-wavelength limit, the dynamics of the wave is found to be governed by a novel nonlinear equation. The result of the moving-frame nonlinear analysis is noteworthy, which shows that this nonlinear equation does have a breather solution and electron viscosity is responsible for the breather. A breather is a nonlinear wave in which energy accumulates in a localized and oscillatory manner. Analytical solution and time-dependent numerical simulation of this novel equation reveal the collapse of a soliton (localized pulse) into a weak noise shelf and formation of shocklike structures.

DOI: [10.1103/PhysRevE.90.063111](https://doi.org/10.1103/PhysRevE.90.063111)

PACS number(s): 52.30.Cv, 52.35.Kt, 52.35.Mw

I. INTRODUCTION

Electron magnetohydrodynamic (EMHD) plasma [1,2] occurs in various physical problem going from the laboratory to space plasma. In EMHD plasma the characteristic frequency is high ($\omega_{ci} \ll \omega \ll \omega_p^2/\omega_{ce}$, where ω_{ce}, ω_{ci} are electron and ion gyrofrequencies and ω_p is electron plasma frequency) and the current flow velocities are larger compared to the mass velocities. In such a plasma electrons take part in the dynamics, whereas comparatively massive ions provide a charge-neutralized static background [1,2]. The characteristic spatial scale lies between electron and ion Larmor radius ($\rho_e \ll \lambda/2\pi \ll \rho_i$) where ρ_e, ρ_i are electron and ion gyroradii, and λ is the typical wavelength. In current plasma physics research, EMHD is of profound interest due to its relevance to both basic plasma physics and its applications. The EMHD also plays an important role in fundamental astrophysical processes like reconnection of magnetic field lines in solar flares [3–7], which are believed to cause a large release of magnetic energy into particle energy. Also EMHD has applications to fast ignition (FI) [8–10], inertial confinement fusion (ICF), laser plasma interaction [11,12], fast Z pinches [13], plasma opening switches [14], and pseudosparks [15].

Various linear and nonlinear EMHD phenomena in plasmas are investigated including the dispersive Whistler wave (a small-amplitude magnetic field fluctuation oscillating above the ion cyclotron frequency [16]). The magnetic drift wave [17], a low-frequency magnetic field fluctuation in the presence of density inhomogeneity oscillating in the frequency regime $\omega < k_{\perp}c, \omega_p, \omega_{ce}$ is obtained with k_{\perp} as the perpendicular wave number, $\omega_p = (4\pi n_{00}e^2/m)^{1/2}$ the electron plasma frequency, $\omega_{ce} = eB_0/mc$ the electron cyclotron frequency, m the electron mass, B_0 the homogeneous magnetic field, and n_{00} the equilibrium density. The nonlinear EMHD activities in plasma arise when the large electron current modifies the properties of background plasma, and the fluctuating field is comparable to the background magnetic field. The nonlinearity in EMHD plasmas triggers interesting physical phenomena such as magnetic field structure formation [18,19],

Weibel instability [20], electron vortex structures [1,21–23], and contributing magnetic turbulence [24–26].

Being a lighter mass compared to ions electrons can be easily accelerated to high energies. These accelerated electrons can be regarded as a source of high energy and may be employed to heat the classical overdense region of the plasma medium. During this process these energetic electrons have to traverse through an inhomogeneous background, and eventually a magnetic drift wave can be excited in such a plasma. Thus the objective of this present work is to investigate by theoretical and computational means the transport dynamics of the nonlinear low-frequency magnetic drift wave in an inhomogeneous plasma in the presence of electron viscosity. Our analysis shows that the dynamics of the wave is governed by a novel nonlinear equation, which is the Korteweg–de Vries–Zakharov–Kuznetsov (KdV-ZK) equation with a higher (fourth) order dissipative term. The analytical solution and time-dependent numerical simulation of this novel equation reveal that a single soliton (localized pulse) first collapses into a weak noise shelf and then forms a shock structure. We also analyze the nonlinear equation in a moving-frame by posing the problem as an autonomous dynamical system. This moving-frame nonlinear analysis confirms the shocklike structures and also predicts the existence of breather solution: a breather is a nonlinear wave in which energy concentrates in a localized and oscillatory fashion. In an EMHD plasma such nonlinear structure is predicted for the first time in the presence of viscosity, which is a novel result in this work. The breather oscillations are attributed through the well-known spatially periodic sine-Gordon equation and nonlinear Schrödinger equation [27–30]. Here we predict that the derived KdV-ZK equation with fourth order dissipation also supports breather oscillations, and here the electron viscosity is responsible for the breather formation.

The paper is organized as follows: In Sec. II we present the nonlinear equation that governs the dynamics of magnetic drift wave in a viscous EMHD plasma. We investigate the solution of the nonlinear equation analytically and numerically

in Sec. III. Section IV deals with the moving-frame analysis of the nonlinear equation. Finally, we conclude with physical applications of our results in Sec. V.

II. NONLINEAR EVOLUTION EQUATION

To formulate the problem and to find the explicit final results, the physical assumptions are as follows:

(i) The plasma is magnetized and inhomogeneous. The magnetic field is in the z direction, and the effects of magnetic geometry are neglected. Only the fluctuations of the axial magnetic field are considered. Here we consider a two-dimensional (2D) slab geometry (i.e., $\partial/\partial z = 0$) system with no variation along the z direction, and thus all the variables are functions of two spatial coordinates (x, y) and time t only.

(ii) We consider that the time scale for electron response is much shorter than ion response time scale, and therefore the ions are considered to be immobile forming a static charge-neutralizing background.

(iii) We assume a low-beta plasma where the magnetic pressure much higher than kinetic pressure the pressure gradient force is ignored. To incorporate the dissipative effects, a phenomenological viscosity (perpendicular to the magnetic field) is considered. The viscosity is used as an effective energy sink [24].

(iv) For the low-frequency [$\omega \ll \min(\omega_p, \omega_p^2/\omega_{ce})$] oscillation, we neglect the displacement current as well as the density fluctuations, which are the EMHD approximation compatible with $\nabla \cdot \mathbf{J} = 0$, where \mathbf{J} is the current density. This EMHD approximation leads us to determine the current by the electron flow velocity \mathbf{v}_e only as the ions are stationary.

On the basis of these facts, we consider the following electron momentum equation:

$$mn \left(\frac{\partial}{\partial t} + \mathbf{v}_e \cdot \nabla \right) \mathbf{v}_e = -ne \left(\mathbf{E} + \frac{1}{c} \mathbf{v}_e \times \mathbf{B} \right) + \mu_e \nabla^2 \mathbf{v}_e, \quad (1)$$

where $m(e)$ is the electron mass (charge), \mathbf{E} is the electric field, \mathbf{B} is the magnetic field, and μ_e is the phenomenological electron viscosity coefficient. The electric field \mathbf{E} in electron momentum equation (1) can be obtained using Faraday's law:

$$\nabla \times \mathbf{E} = -\frac{1}{c} \frac{\partial \mathbf{B}}{\partial t}. \quad (2)$$

Dividing Eq. (1) by mn taking the curl and using Eq. (2), we get the following self-consistent nonlinear electron vorticity equation:

$$\left(\frac{\partial}{\partial t} + \mathbf{v}_e \cdot \nabla \right) (\boldsymbol{\Omega} - \boldsymbol{\Omega}_c) + [\nabla \cdot \mathbf{v}_e] (\boldsymbol{\Omega} - \boldsymbol{\Omega}_c) = [(\boldsymbol{\Omega} - \boldsymbol{\Omega}_c) \cdot \nabla] \mathbf{v}_e + \mu \nabla^2 \boldsymbol{\Omega}, \quad (3)$$

where $\boldsymbol{\Omega} = \nabla \times \mathbf{v}_e$ is the electron vorticity, $\mu = \mu_e/mn$ is the kinematic viscosity, and $\boldsymbol{\Omega}_c = e\mathbf{B}/cm$ is the cyclotron vorticity. Because of the physical assumption (iv) from Ampere's law, we obtain the following expression of electron velocity:

$$\mathbf{v}_e = -\frac{c \nabla \times \mathbf{B}}{4\pi en}, \quad (4)$$

where n is the electron number density. The EMHD theory describes the dynamics of magnetized electrons in the presence of both a self-generated and an externally applied magnetic field [1]. Therefore, the magnetic field \mathbf{B} can be written in the form

$$\mathbf{B} = \hat{e}_z [B_0 + \tilde{b}(x, y, t)] \text{ so that } \nabla \times \mathbf{B} = -\hat{e}_z \times \nabla \tilde{b}, \quad (5)$$

where B_0 is the average homogeneous magnetic field and \tilde{b} is the fluctuating magnetic field. In EMHD, normally density fluctuations are ignored, therefore n is only equilibrium density. Equations (3)–(5) are basic equations that describe waves in an inhomogeneous EMHD plasma.

To write equations in dimensionless form we use a time scale as $L_n^2/\delta_e V_A$ (where $\delta_e = c/\omega_p$ is the electron skin depth and $V_A = B_0/\sqrt{4\pi n_0 m}$ is the electron Alfvén velocity), a typical field intensity B_0 , and a typical inhomogeneous spatial scale length L_n . Then eliminating \mathbf{v}_e from the vorticity equation with the help of Eq. (4), we finally obtain the leading order nonlinear dimensionless electron vorticity equation [17]:

$$\left(\frac{\partial}{\partial t} + \hat{e}_z \times \nabla_{\perp} b \cdot \nabla_{\perp} \right) \left[b - \left(\frac{\delta_e}{L_n} \right)^2 \nabla_{\perp}^2 b \right] + \frac{\partial b}{\partial y} + \left[b - \left(\frac{\delta_e}{L_n} \right)^2 \nabla_{\perp}^2 b \right] \frac{\partial b}{\partial y} = -\mu \left(\frac{\delta_e}{L_n} \right)^2 \nabla_{\perp}^2 \nabla_{\perp}^2 b, \quad (6)$$

where $\nabla_{\perp} = \hat{e}_x \partial/\partial x + \hat{e}_y \partial/\partial y$, $b \equiv \tilde{b}/B_0$, and $\mu \equiv \mu/(\delta_e V_A)$. In this equation, the axial field fluctuation b acts like a stream function of the electron flow $\hat{e}_z \times \nabla_{\perp} b$. Equation (6) is the governing equation of the magnetic field fluctuations for the low-frequency nonlinear wave in inhomogeneous EMHD plasmas in the presence of electron viscous diffusion.

To study the linear properties of this equation, first, we switch off the nonlinear terms in Eq. (6) and obtain the linear equation

$$\frac{\partial}{\partial t} \left[b - \left(\frac{\delta_e}{L_n} \right)^2 \nabla_{\perp}^2 b \right] + \frac{\partial b}{\partial y} = -\mu \left(\frac{\delta_e}{L_n} \right)^2 \nabla_{\perp}^2 \nabla_{\perp}^2 b. \quad (7)$$

Assuming the Fourier mode solution of the magnetic field perturbation $b \sim \exp[-i(\omega t - \mathbf{k} \cdot \mathbf{r})]$, we obtain from Eq. (7) the real (ω_r) and imaginary (ω_i) parts of the frequency ω as follows:

$$\omega_r = \frac{k_y}{1 + k_{\perp}^2} \quad \text{and} \quad \omega_i = -\frac{\mu k_{\perp}^4}{1 + k_{\perp}^2},$$

where $k_{\perp}^2 = k_x^2 + k_y^2$. Since $\omega_i < 0$ the mode is damped, and the expression for ω_i suggests that this damping is due to the viscous diffusion of electrons. In dimensional form ω_r reads as

$$\omega_r = \frac{\omega^*}{1 + k_{\perp}^2 \delta_e^2}$$

where $\omega^* = k_y \delta_e V_A/L_n$ is the drift frequency. The expression of the real frequency given above clearly shows that the low-frequency magnetic drift wave is dispersive in nature and also identifies two scale length regimes of interest: the long-wavelength regime $k_{\perp} \delta_e < 1$ and short-wavelength regime $k_{\perp} \delta_e > 1$. However, here we concentrate on the long-wavelength regime to study the nonlinear properties of the dispersive magnetic drift wave. For the finite amplitude

nonlinear wave, we consider that the electron skin depth δ_e is smaller than the spatial inhomogeneity length L_n so that $\delta_e/L_n < 1$. This permits us to take $\delta_e^2/L_n^2 = \epsilon (\ll 1)$, which defines the strength of the field variables. For the usual perturbation analysis, we take ϵ as the perturbation parameter and introduce the following space coordinates (ξ, η) and slow time scale (τ) :

$$\xi = \frac{1}{2}(y - t), \quad \eta = \frac{1}{2}x \quad \text{and} \quad \tau = \frac{1}{2}\epsilon t.$$

The field variable b is then represented in terms of the small parameter ϵ as $b = \epsilon\phi$. Substituting all these in Eq. (6), the lowest order approximation finally yields the following nonlinear equation in two spatial dimension:

$$\begin{aligned} \frac{\partial\phi}{\partial\tau} + \phi \frac{\partial\phi}{\partial\xi} + \frac{1}{4} \frac{\partial}{\partial\xi} \left(\frac{\partial^2}{\partial\xi^2} + \frac{\partial^2}{\partial\eta^2} \right) \phi \\ + \frac{\mu}{8} \left(\frac{\partial^2}{\partial\xi^2} + \frac{\partial^2}{\partial\eta^2} \right)^2 \phi = 0. \end{aligned} \quad (8)$$

In the absence of electron viscosity ($\mu = 0$), we recover the well-known Korteweg-de Vries-Zakharov-Kuznetsov (KdV-ZK) equation in two dimensions, which exhibits a soliton solution. The analytical solution and its stability are discussed in detail in Ref. [31]. For oblique propagation in two dimensions, we denote $\zeta = \xi + \alpha\eta$, where α is the wave inclination in the ξ - η plane. Then Eq. (8) reduces to the following equation:

$$\frac{\partial\phi}{\partial\tau} + \phi \frac{\partial\phi}{\partial\zeta} + \beta \frac{\partial^3\phi}{\partial\zeta^3} + \nu \frac{\partial^4\phi}{\partial\zeta^4} = 0, \quad (9)$$

where

$$\beta = \frac{1 + \alpha^2}{4} \quad \text{and} \quad \nu = \frac{\mu(1 + \alpha^2)^2}{8}. \quad (10)$$

The presence of viscosity introduces a dissipative effect in the system that can be seen from the term ν . The solutions of this equation are interesting and applicable in different fields of physics and mathematics as described below.

First, to reduce the number of parameters of Eq. (9), we introduce the rescaling as $\phi = 6\beta^{1/3}\bar{\phi}$, $\zeta = \beta^{1/3}\bar{\zeta}$, and $\varepsilon = \nu/\beta^{4/3}$. These transformations turn Eq. (9) into (omitting the bars)

$$\frac{\partial\phi}{\partial\tau} + 6\phi \frac{\partial\phi}{\partial\zeta} + \frac{\partial^3\phi}{\partial\zeta^3} + \varepsilon \frac{\partial^4\phi}{\partial\zeta^4} = 0. \quad (11)$$

Here ε represents the effect of electron viscous diffusion. In the absence of this effect, i.e., if $\varepsilon = 0$, we recover the well-known KdV equation. Here we must emphasize that the KdV equation was derived in a fluid system (water waves) and its solution, soliton, is applicable in nearly all branches of physics. Since dissipation is inherently present in almost every physical system, therefore dissipation-modified KdV should be applicable mostly to all physical systems where such equations arise.

III. SOLUTION IN A WAVE FRAME

First, at the simplest level, we present an exact solution of the Eq. (11) in a frame moving with the phase velocity of the wave. We hope that this will improve our understanding of the behavior of the nonlinear system [Eq. (11)]. To

investigate the nonlinear solution, we transform Eq. (11) into the moving frame $\chi = \zeta - M\tau$, where M is the Mach number (normalized phase velocity). Then integrating the transformed equation once subject to the boundary conditions $\phi \rightarrow 0$, all derivatives $\rightarrow 0$ as $\chi \rightarrow \infty$, and we finally obtain the following nonlinear ordinary differential equation:

$$\varepsilon \frac{d^3\phi}{d\chi^3} + \frac{d^2\phi}{d\chi^2} + 3\phi^2 - M\phi = 0. \quad (12)$$

A. Nonlinear analysis in the absence of electron diffusion

For a nonlinear analysis, first, we neglect the electron diffusion term ($\varepsilon = 0$) in Eq. (11), which then reduces to the usual KdV equation, and the corresponding nonlinear ordinary differential equation (12) becomes

$$\frac{d^2\phi}{d\chi^2} + 3\phi^2 - M\phi = 0. \quad (13)$$

Next we recast the nonlinear equation (13) in the following two simultaneous equations:

$$\frac{d\phi}{d\chi} = \psi, \quad \frac{d\psi}{d\chi} = M\phi - 3\phi^2. \quad (14)$$

In the ϕ - ψ plane, this dynamical system has the following two physically possible equilibrium (stationary) points:

$$(0,0) \quad \text{and} \quad \left(\frac{M}{3}, 0\right).$$

To investigate the nature of these two stationary points, we calculate the variational matrix of the system (14) at these two stationary points. These matrices are as follows:

$$J_{(0,0)} = \begin{bmatrix} 0 & 1 \\ M & 0 \end{bmatrix}, \quad J_{(M/3,0)} = \begin{bmatrix} 0 & 1 \\ -M & 0 \end{bmatrix}. \quad (15)$$

The corresponding pair of eigenvalues are determined from the following characteristic (quadratic) equations:

$$\gamma_{(0,0)}^2 - M = 0 \quad \text{and} \quad \gamma_{(M/3,0)}^2 + M = 0, \quad (16)$$

which are $\pm\sqrt{M}$ (real and distinct) and $\pm i\sqrt{M}$ (purely imaginary), respectively. Thus the stationary point $(0,0)$ is a saddle point, and the stationary point $(M/3,0)$ is a center or elliptic fixed point.

Then we solve the dynamical system (14) for $M = 4$ with $(0,0)$ and $(M/3,0)$ as the initial conditions by the Runge-Kutta-Fehlberg (RKF) method. The solutions are shown graphically in Figs. 1 and 2. The phase-space trajectories in the ϕ - ψ plane of the dynamical system (14) are shown graphically in Fig. 1. Figure 1(a) shows that a small perturbation around the equilibrium point $(0,0)$ (saddle point) forms a homoclinic orbit (separatrix) in the ϕ - ψ plane, which is the signature of the soliton solution. On the other hand, Fig. 1(b) shows the elliptic orbit with center at $(M/3,0)$ in the ϕ - ψ plane, which is the signature of the oscillatory solution. Figures 2(a) and 2(b) confirm the soliton solution and also the oscillatory solution of the system (14).

In the next section, we investigate how the electron viscosity affects the nonlinear dynamics of the system.

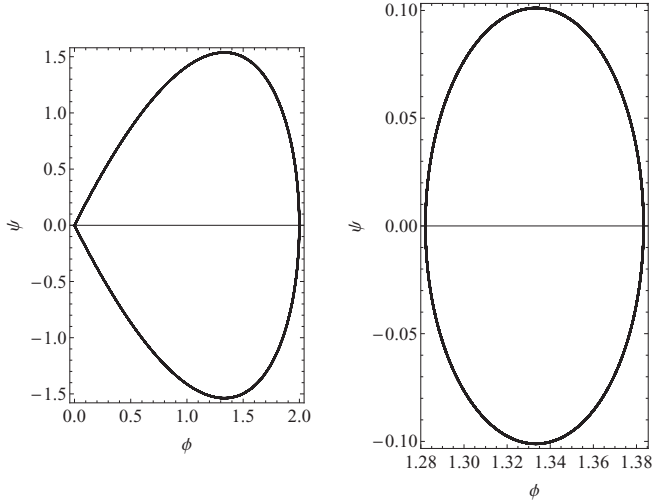


FIG. 1. Phase-space trajectories in the ϕ - ψ plane of the dimensionless dynamical system (14) with $M = 4$. (a) Homoclinic orbit of a small disturbance around the stationary point $(0,0)$. (b) Elliptic orbit of a small disturbance around the stationary point $(M/3,0)$.

B. Nonlinear analysis in the presence of electron diffusion

Here we investigate the effects of electron viscosity on the dynamical behavior of the nonlinear equation (11). Therefore, we recast the nonlinear equation (12) in the following three simultaneous equations:

$$\begin{aligned} \frac{d\phi}{d\chi} &= \psi, & \frac{d\psi}{d\chi} &= \varphi, \\ \frac{d\varphi}{d\chi} &= \left(\frac{M}{\varepsilon}\right)\phi - \left(\frac{3}{\varepsilon}\right)\phi^2 - \left(\frac{1}{\varepsilon}\right)\varphi. \end{aligned} \quad (17)$$

In the ϕ - ψ - φ hyperplane, this dynamical system has the following two physically possible equilibrium (stationary) points:

$$(0,0,0) \quad \text{and} \quad \left(\frac{M}{3},0,0\right).$$

To study the nature of these stationary points, we calculate the variational matrix of the system (17) at these two stationary

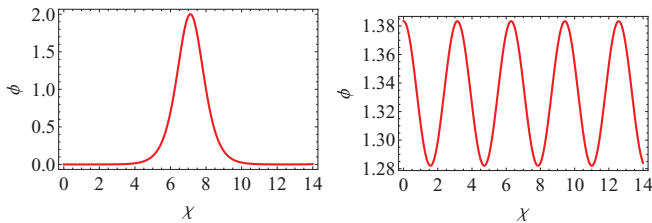


FIG. 2. (Color online) Numerical solution of the dynamical system (14) with $M = 4$. (a) Formation of a soliton of a dimensionless small disturbance around the stationary point $(0,0)$. (b) Oscillatory solution of a dimensionless small disturbance around the stationary point $(M/3,0)$.

points. These matrices are as follows:

$$\begin{aligned} J_{(0,0,0)} &= \begin{bmatrix} 0 & 1 & 0 \\ 0 & 0 & 1 \\ \frac{M}{\varepsilon} & 0 & -\frac{1}{\varepsilon} \end{bmatrix}, \\ J_{(\frac{M}{3},0,0)} &= \begin{bmatrix} 0 & 1 & 0 \\ 0 & 0 & 1 \\ -\frac{M}{\varepsilon} & 0 & -\frac{1}{\varepsilon} \end{bmatrix}. \end{aligned} \quad (18)$$

The eigenvalues of these variational matrices are given by the following characteristic (cubic) equations:

$$\varepsilon\lambda^3 + \lambda^2 - M = 0 \quad \text{and} \quad \varepsilon\Lambda^3 + \Lambda^2 + M = 0, \quad (19)$$

where λ and Λ are the eigenvalues corresponding to the stationary points $(0,0,0)$ and $(M/3,0,0)$. Note that in the absence of ε , the three-dimensional dynamical system (17) reduces to a 2D system (14), and as a consequence the characteristic equations (19) become identical with that for the KdV equation (16). Thus presence of electron viscosity does modify the eigenvalues. Let us check how it changes the character of the eigenvalues. The eigenvalues of Eq. (19) for $\varepsilon = 0.1$ and $M = 4$ are as follows:

$$\begin{aligned} \begin{bmatrix} \lambda_1 \\ \lambda_2 \\ \lambda_3 \end{bmatrix} &= \begin{bmatrix} -9.56 \\ -2.28 \\ 1.84 \end{bmatrix} \quad \text{and} \\ \begin{bmatrix} \Lambda_1 \\ \Lambda_2 \\ \Lambda_3 \end{bmatrix} &= \begin{bmatrix} -10.37 \\ 0.19 + 1.95 i \\ 0.19 - 1.95 i \end{bmatrix}. \end{aligned}$$

These sets of eigenvalues clearly demonstrate that the stationary point $(0,0,0)$ is a saddle node, whereas the stationary point $(M/3,0,0)$ is a saddle focus as the pair of conjugate eigenvalues have a positive real part. It is interesting to note that in the case of KdV eigenvalues, the stationary point $(M/3,0)$ is a center as the pair of conjugate eigenvalues are purely imaginary [roots of second equation of (16)]. Thus, the presence of electron viscosity indeed changes the character of the eigenvalues and leads to new interesting features of the solution of the system (17).

Let us apply the Shilnikov's criteria [32] for the existence of a stable periodic orbit of the system around the stationary point $(M/3,0,0)$. For this we calculate the saddle value $\sigma [=2 \times \text{Re}(\Lambda) + \Lambda_1] < 0$, and according to the criteria, the system has a stable periodic orbit in the small neighborhood of $(M/3,0,0)$.

Next we solve the dynamical system (17) by the RKF method by taking the stationary point $(0,0,0)$ as the initial condition with $\varepsilon = 0.1$ and $M = 4$. Then starting from a small perturbation of the initial condition $(0,0,0)$ and upon numerical integration of the dynamical system, it is seen that the perturbation develops into a shocklike structure as illustrated in Fig. 3(a) with an oscillating transition corresponding to the second stationary point $(M/3,0,0)$. The projection of the phase-space trajectory on the ϕ - ψ plane of the dynamical system (17) is shown graphically in Fig. 3(b). This phase-space trajectory clearly shows a stable closed periodic orbit around the stationary point $(M/3,0,0)$.

Finally we solve the dynamical system (17) by the RKF method with the stationary point $(M/3,0,0)$ as the initial

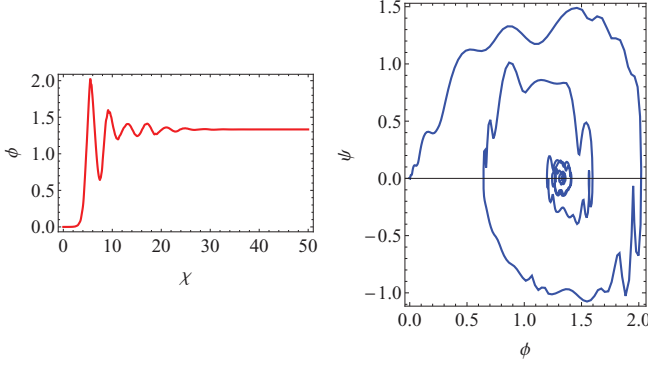


FIG. 3. (Color online) Numerical solution of the dimensionless dynamical system (17) with $\varepsilon = 0.1$, $M = 4$, and $(0,0,0)$ as the initial condition. (a) Formation of a shocklike structure for ϕ (dimensionless magnetic field fluctuations) with moving frame χ . (b) Projection of the phase portrait trajectory of (17) in the ϕ - ψ plane.

condition for two sets of parameters: $\varepsilon = 0.5$, $M = 2$ and $\varepsilon = 1$, $M = 4$. The corresponding eigenvalues are

$$\begin{aligned} \begin{bmatrix} \Lambda_1 \\ \Lambda_2 \\ \Lambda_3 \end{bmatrix}_{(\varepsilon=0.5, M=2)} &= \begin{bmatrix} -2.59 \\ 0.3 + 1.2i \\ 0.3 - 1.2i \end{bmatrix} \quad \text{and} \\ \begin{bmatrix} \Lambda_1 \\ \Lambda_2 \\ \Lambda_3 \end{bmatrix}_{(\varepsilon=1, M=4)} &= \begin{bmatrix} -2 \\ 0.5(1 + i\sqrt{7}) \\ 0.5(1 - i\sqrt{7}) \end{bmatrix}. \end{aligned} \quad (20)$$

These values again satisfy Shilnikov's condition for the stable periodic orbit of the dynamical system (17) in the vicinity of the saddle focus $(M/3, 0, 0)$. As a consequence, a small perturbation around this stationary point develops into a breather solution as illustrated in Fig. 4. A breather is a nonlinear wave in which energy concentrates in a localized and oscillatory manner. It is a localized periodic solution of a nonlinear system. A breather is described as an oscillatory solution (wave packet) about a stationary point whose envelope and oscillatory part move with different velocities [33]. One breather is determined by a couple of complex conjugated eigenvalues, and therefore it is a two-parameter solution (nonzero real and imaginary parts of Λ) which in general behaves like a wave packet. We can see from the computation and also the character of the eigenvalues (20) of the dynamical system (17) that indeed the solutions represented in Fig. 4 resemble the situation of a breather. The electron viscous

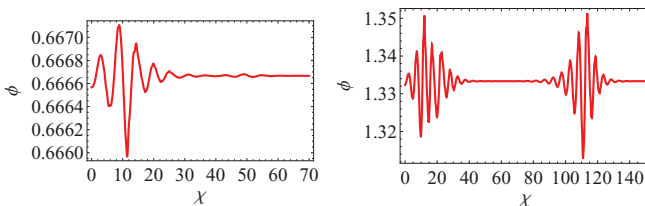


FIG. 4. (Color online) Breather solutions of the dimensionless dynamical system (17) with $(M/3, 0, 0)$ as the initial condition. (a) Single breather for $\varepsilon = 0.5$, $M = 2$. (b) Multiple breather for $\varepsilon = 1$, $M = 4$.

diffusion is responsible for this breather solution because of the fact that electron viscous term is responsible for the nonzero real part of the complex conjugated eigenvalues. In the absence of this electron viscosity we have only purely imaginary eigenvalues, which corresponds to the oscillatory solution [Fig. 2(b) as in case of KdV equation].

IV. COLLAPSE OF A SOLITON INTO A NOISE SHELF AND FORMATION OF SHOCK STRUCTURES

A. Analytical solution

The KdV equation is a completely integrable Hamiltonian system for an infinite set of conservation laws [34]. These conservation laws (integrals of motion) are essential to study the propagation dynamics as well as the localized structures formed by the nonlinear evolution equation. In the case of $\varepsilon = 0$, a solution of Eq. (11), satisfying the boundary conditions $\phi(\zeta, \tau) \rightarrow 0$ at $|\zeta| \rightarrow \infty$, has a soliton form $\phi(\zeta, \tau) = 2\kappa^2 \text{sech}^2 \kappa(\zeta - V\tau)$, where V is the soliton velocity, $2\kappa^2$ is the soliton amplitude, and κ^{-1} is the width of the soliton. However, here we investigate the solution (if it exists) of Eq. (11) in the presence of finite (but small) ε using the same boundary conditions at $|\zeta| \rightarrow \infty$. In the presence of weak dissipation, one can obtain an approximate solution by the soliton perturbation analysis [35]. Actually, a weak perturbation has a small influence on the formation of solitons, and as a consequence one can treat solitons as noninteracting and hence can find, as a first approximation, the influence of perturbation on a single soliton. Here we adopt this perturbation procedure to find an approximate time evolution solution of Eq. (11) with $\varepsilon \ll 1$ as the perturbed parameter. To apply this perturbation, we consider the following perturbed single soliton solution described by

$$\begin{aligned} \phi(\zeta, \tau) &= \phi_s[\kappa(\tau), \theta(\tau)] + \delta\phi(\zeta, \tau), \\ &= 2\kappa^2(\tau) \text{sech}^2 \Theta(\tau) + \delta\phi(\zeta, \tau), \end{aligned} \quad (21)$$

where $\Theta(\tau) = \kappa(\tau)[\zeta - \theta(\tau)]$, $d\theta(\tau)/d\tau$ is the soliton velocity, and $\delta\phi$ is the perturbed soliton. Actually, one of the important results of the soliton perturbation is the generation of a “tail”: a wave packet of small amplitude following behind, or, in some cases, in front of, a soliton [35]. The length of the “tail” increases approximately with time, and as a result it spreads with time. The “tail” may contain “energy” and “momentum” comparable to and even larger than those of solitons [35]. Once the “tail” is formed, it becomes disconnected from its “mother-soliton” kinetics and transforms into a “noise shelf” [36]. This $\delta\phi$ gives the analytical expression for the “tail part” of the soliton given by

$$\begin{aligned} \phi_{\text{tail}} &= \lim_{\zeta \rightarrow -\infty} \delta\phi \\ &\equiv -\frac{\varepsilon}{4\kappa^3(\tau)} \int_{-\infty}^{\infty} \frac{\partial^4 \phi_s}{\partial \zeta^4} \tanh^2 \Theta(\tau) d\zeta = \left(\frac{32}{21}\right) \varepsilon \kappa^2(\tau). \end{aligned} \quad (22)$$

We know that to explain the effects of disturbance (here dissipation) on the initial soliton (leading order), the judicious choice is the use of conservation laws [36]. Thus to find the analytical expression for $\kappa(\tau)$, we consider the energy

conservation law of Eq. (11), which reads as

$$\frac{\partial \mathcal{E}}{\partial t} = -\varepsilon \int_{-\infty}^{\infty} \left(\frac{\partial^2 \phi_s}{\partial \zeta^2} \right)^2 d\zeta, \quad \mathcal{E} \equiv \int_{-\infty}^{\infty} \frac{1}{2} \phi_s^2 d\zeta. \quad (23)$$

Finally substitution of (21) in Eq. (23) yields the following expressions for soliton amplitude and energy:

$$\begin{aligned} \kappa^2(\tau) &= \kappa^2(0) \left[1 + \left(\frac{1040}{21} \right) \varepsilon \tau \kappa^4(0) \right]^{-1/2}, \\ \mathcal{E} &= \left(\frac{8}{3} \right) \kappa^3(0) \left[1 + \left(\frac{1040}{21} \right) \varepsilon \tau \kappa^4(0) \right]^{-3/4}. \end{aligned} \quad (24)$$

These clearly show that the viscosity-induced dissipation causes the soliton amplitude and energy to decay algebraically with time τ . It is interesting to note that the total soliton mass is conserved: $\int_{-\infty}^{\infty} \phi_s d\zeta = 0$, because the matter ejected from the damping soliton encounters a phase transition between the ‘‘soliton state’’ and ‘‘noise state’’ that allows the necessary mass conservation.

Note that the above solution is the approximated (leading order) solution of Eq. (9) [rescaled Eq. (11)], and higher order terms in the perturbation analysis introduce only corrections (the change in amplitude, velocity, and width remain the same as obtained in the leading order approximation) [35].

B. Time-dependent numerical simulation

In the previous section, we have seen that the exact solution of Eq. (11) is not possible, but one can find approximate solution by treating the equation as a perturbed KdV equation. However, in this section we numerically simulate the nonlinear equation (9) using a MATHEMATICA-based finite difference scheme. For the time-dependent numerical solution, we use the soliton solution as the initial waveform: $\phi(\zeta, 0) = 3U \operatorname{sech}^2(\sqrt{U/4\beta}\zeta)$, $\zeta \in [-L, L]$, where L is approximately the system size. The boundary conditions are $\phi(\pm L, \tau) = 3U \operatorname{sech}^2(\pm\sqrt{U/4\beta}L)$ and $\phi_\zeta(-L, \tau) = 0 = \phi_\zeta(L, \tau)$. To obtain adequate results through computation, we take $L = 40$ and $U = 1$. The time-dependent numerical solutions are shown in Fig. 5. These solutions show the decrease of soliton amplitude (and increase of width) due to the presence of dissipation and also clearly demonstrate the formation of soliton noise-tail structures at different time. Finally, a shock structure is seen to be formed [Fig. 5(b)]. Thus, the time-dependent numerical solutions agree well with the preceding time-dependent analytical analysis.

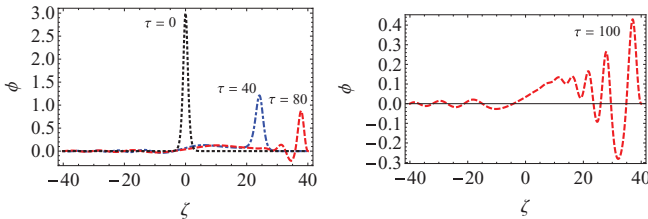


FIG. 5. (Color online) Time-dependent numerical solution of (9) with soliton solution as an initial profile. The physical parameters are $\mu = 0.2$, $\alpha = 0.1$, and $U = 1$. (a) Decreasing soliton amplitude and noise-tail formation at $\tau = 40$ and $\tau = 80$. (b) Oscillatory shock structure is formed at $\tau = 100$.

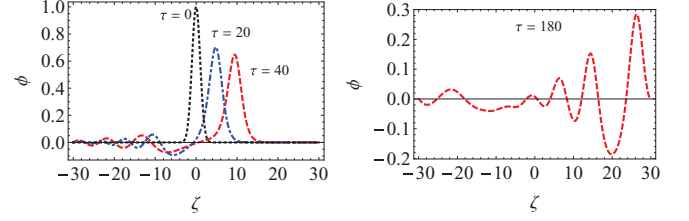


FIG. 6. (Color online) Time-dependent numerical solution of (9) with Gaussian initial profile $\phi(\zeta, 0) = \exp(-\zeta^2/2)$. (a) Decreasing amplitude and formation of noise tails at $\tau = 20$ and $\tau = 40$. (b) Oscillatory shock structure is formed at $\tau = 180$. In the simulation the physical parameters are as in Fig. 5.

To confirm our simulation result, we also simulate Eq. (9) with different initial condition; namely, we use a Gaussian profile $\phi(\zeta, 0) = \exp(-\zeta^2/2)$ $\zeta \in [-L, L]$ as the initial profile. The boundary conditions are as before $\phi(\pm L, \tau) = \exp[-(\pm L)^2/2]$ and $\phi_\zeta(-L, \tau) = 0 = \phi_\zeta(L, \tau)$ with $L = 30$. The solutions are depicted in Fig. 6. The figure again shows that due to the presence of dissipation, first noise tails are formed at slower time and then as time passes shock structures are formed. All these time-dependent numerical solutions again confirm the shock solution of Eq. (9).

V. DISCUSSION

The nonlinearity of a physical system manifests itself in the form of coherent complex structures. These structures are best understood by the analytical solutions and numerical simulations of the dynamical equations. Therefore, in the present work, we investigate the nonlinear structure of a low-frequency wave in a 2D EMHD plasma in the presence of electron viscosity. The dynamics of the nonlinear wave is shown to be governed by a nonlinear equation. This nonlinear equation is the KdV-ZK equation with a higher (fourth) order dissipative term that arises due to the electron viscosity.

First, at the simplest level, we analyze the nonlinear system in a moving frame by posing the problem as an autonomous dynamical system. Our analysis predicts the formation of breathers that have solitonic structures. In the present situation the breather solution is a nonlinear traveling wave. Apart from this the standing breathers correspond to localized solutions whose amplitude varies in time (they are sometimes called oscillons). The breather solution presented here is a novel nonlinear structure in a magnetized electron plasma, besides the usual shock structure. Furthermore, this novel equation is analyzed analytically with the help of the dissipative perturbation technique and also by the time-dependent numerical simulation. The analytical and simulation results reveal that a single solitonic or Gaussian pulse first collapses into a weak noise shelf, and then it forms shock structure in EMHD plasma. The observed shock is compressive in nature, and the total dissipated energy estimate associated with the shock can be written as

$$Q \sim \varepsilon \int \left(\frac{\partial^2 \phi}{\partial \zeta^2} \right)^2 d\zeta L \sim \varepsilon \frac{\phi^2}{\Delta^3} L.$$

Here L and Δ are the typical (normalized) distance traversed in the inhomogeneity layer and the (normalized) shock width. Using Ampère's law (4), we can express the magnetic field fluctuation $b(\sim \phi)$ in terms of the typical incoming current filament dimension a and the electron velocity v_e . Thus $\phi \sim av_e$ and the total dissipated energy then becomes

$$Q \sim \varepsilon \frac{a^2 v_e^2}{\Delta^3} L.$$

This process of collisionless electron energy dissipation and the variation of the electron velocity (magnetic field fluctuations) resulting from propagation of compressional shock waves is of significant importance in the FI experiments [9], which is a simple variant of the ICF technique. The electrons are energized by the passing of the shock wave due to the conversion of wave energy into particle kinetic energy, which drives the particle acceleration. As a result, the electrons can be good source of energy for plasma heating, and the high-energy electrons can penetrate the high-density overdense

region, which is not accessible by the laser fields. Thus, these high-energy collisionless electrons can also be employed for creating an ignition spark in FI experiments [9].

The breather oscillation is the outcome of interactions between two-phase waves. So the formation of breather is the signature of the phase mixing of waves. Similar types of phenomena (wave synchronization) of typical magnetic field fluctuations from repeated discharge pulses are observed in the EMHD plasma experiment [37]. This is the signature of the experimentally observed breather-like structures in EMHD plasma. Moreover, the observed breather-like localized structures in EMHD plasma exchange energy between the structure and the plasma. Thus the breather-like solution is also applicable to the penetration of electrons into the overdense plasma in the FI experiments in ICF.

Finally, EMHD plays an important role in magnetic confinement plasmas as well as in space plasmas. Thus, the results of the present investigations could be useful to understand the physics of electron transport phenomena in laboratory and space plasmas.

-
- [1] A. S. Kingsep, K. V. Chukbar, and V. V. Yankov, *Reviews of Plasma Physics* (Consultant Bureau, New York, 1990), Vol. 16.
- [2] A. V. Gordeev, A. S. Kingsep, and L. I. Rudakov, *Phys. Rep.* **243**, 215 (1994).
- [3] D. Biskamp, E. Schwarz, and J. F. Drake, *Phys. Rev. Lett.* **76**, 1264 (1996).
- [4] D. Biskamp, in *Magnetic Reconnection in Plasmas* (Cambridge University Press, Cambridge, England, 2000), p. 206.
- [5] E. Priest and T. Forbes, in *Magnetic Reconnection: MHD Theory and Applications* (Cambridge University Press, Cambridge, England, 2000), p. 38.
- [6] L. I. Rudakov and J. D. Huba, *Phys. Rev. Lett.* **89**, 095002 (2002).
- [7] E. R. Priest, *Earth Planets Space* **53**, 483 (2001).
- [8] R. Kodama *et al.*, *Nature (London)* **418**, 933 (2002); M. H. Key, *ibid.* **412**, 775 (2001).
- [9] M. Tabak, I. Hammer, M. E. Glinsky *et al.*, *Phys. Plasmas* **1**, 1626 (1994).
- [10] K. A. Tanaka, R. Kodama, K. Mima *et al.*, *Phys. Plasmas* **10**, 1925 (2003).
- [11] W. L. Kruer, *Physics of LPlasma Interaction* (Addison-Wesley, New York, 1988).
- [12] P. H. Diamond, A. Hasegawa, and K. Mima, *Plasma Phys. Control. Fusion* **53**, 124001 (2011).
- [13] J. F. Drake, D. Biskamp, and A. Zieler, *Geophys. Res. Lett.* **24**, 2921 (1997).
- [14] B. V. Weber, R. J. Comisso, P. J. Goodrich, J. M. Grossman, D. D. Hinshelwood, P. F. Ottinger, and B. S. Swanekamp, *Phys. Plasmas* **2**, 3893 (1995).
- [15] K. Frank and J. Christiansen, *IEEE Trans. Plasma Sci.* **17**, 748 (1989).
- [16] R. A. Helliwell, *Whistlers and Related Ionospheric Plasma* (Stanford University Press, Stanford, CA, 1965).
- [17] N. Chakrabarti and R. Singh, *Phys. Plasmas* **11**, 5475 (2004).
- [18] R. L. Stenzel and J. M. Urrutia, *Phys. Rev. Lett.* **81**, 2064 (1998).
- [19] G. Ravi, S. K. Matto, L. M. Awasthi, and V. P. Anitha, *Phys. Plasmas* **10**, 2194 (2003).
- [20] V. Yu Bychenkov, V. P. Silin, and V. T. Tikhonchuk, *Sov. Phys. JETP* **71**, 709 (1990).
- [21] V. I. Petviashvili and V. V. Yankov, *Reviews of Plasma Physics* (Consultant Bureau, New York, 1989), Vol. 14.
- [22] J. Nycander, V. P. Pavlenko, and L. Stenflo, *Phys. Fluids* **30**, 1367 (1987).
- [23] L. Stenflo, P. K. Shukla, G. Murtaza, and M. Y. Yu, *Contr. Plasma Phys.* **30**, 407 (1990).
- [24] D. Biskamp, E. Schwarz, A. Zeiler, A. Celani, and J. F. Drake, *Phys. Plasmas* **6**, 751 (1999).
- [25] S. Dastgeer and G. P. Zank, *Astrophys. J.* **599**, 715 (2003).
- [26] D. Shaikh and G. P. Zank, *Phys. Plasmas* **12**, 122310 (2005).
- [27] L. Friedland and A. G. Shagalov, *Phys. Rev. E* **71**, 036206 (2005).
- [28] L. Friedland and A. G. Shagalov, *Phys. Rev. E* **73**, 066612 (2006).
- [29] V. Koukoulouyannis and I. Kourakis, *Phys. Rev. E* **76**, 016402 (2007).
- [30] T. E. Sheridan, *Phys. Rev. E* **72**, 026405 (2005).
- [31] S. Ghosh and N. Chakrabarti, *Plasma Phys. Control. Fusion* **55**, 035008 (2013).
- [32] L. P. Shilnikov, A. Shilnikov, D. Turaev, and L. Chua, *Methods of Qualitative Theory in Nonlinear Dynamics: Parts I and II* (World Scientific, Singapore, 1998).
- [33] G. L. Lamb, *Elements of Soliton Theory* (Wiley, New York, 1980).
- [34] V. Yu. Belashov and S. V. Vladimirov, *Solitary Waves in Dispersive Complex Media* (Springer-Verlag, Berlin, 2005).
- [35] V. I. Karpman and E. M. Maslov, *Sov. Phys. JETP* **46**, 281 (1977); **48**, 252 (1978).
- [36] A. C. Newell, *Solitons in Mathematics and Physics* (SIAM, Philadelphia, 1985).
- [37] R. L. Stenzel and J. M. Urrutia, *Phys. Plasmas* **7**, 4466 (2000).